

trans-Difluorosilicon(IV) Complexes of Tetra-*p*-tolylporphyrin and Tetrakis(*p*-(trifluoromethyl)phenyl)porphyrin: Crystal Structures and Unprecedented Reactivity in Hexacoordinate Difluorosilanes¹

Kevin M. Kane[†] and Frederick R. Lemke*

Department of Chemistry, Ohio University, Athens, Ohio 45701-2979

Jeffrey L. Petersen[‡]

Department of Chemistry, West Virginia University, Morgantown, West Virginia 26506

Received May 30, 1996[⊗]

Single-crystal X-ray structures have been determined for the difluoro(porphyrinato)silicon(IV) complexes *trans*-(Por)SiF₂ (Por = the dianions of tetra-*p*-tolylporphyrin (TTP) and tetrakis(*p*-(trifluoromethyl)phenyl)porphyrin). Crystallographic data for (TTP)SiF₂·Et₂O: monoclinic, space group *C2/c*, *a* = 30.228(4) Å, *b* = 9.913(4) Å, *c* = 15.474(5) Å, $\alpha = \gamma = 90^\circ$, $\beta = 114.58(3)^\circ$, *V* = 4217(2) Å³, *Z* = 4, *R*₁ = 0.0588. Crystallographic data for (TTFP)SiF₂: monoclinic, space group *C2/c*, *a* = 31.557(2) Å, *b* = 9.546(1) Å, *c* = 15.941(1) Å, $\alpha = \gamma = 90^\circ$, $\beta = 115.83(1)^\circ$, *V* = 4322.4(8) Å³, *Z* = 4, *R*₁ = 0.0489. In both structures, the silicon lies in a slightly distorted octahedral geometry (average distances: Si–F 1.642 Å and Si–N 1.919 Å) with the fluorides in a *trans* configuration, and the porphyrin is in a *ruf* nonplanar form. The *trans*-(Por)SiF₂ structures were compared to the structures of related hexacoordinate *cis*-difluorosilanes and other group 14 metalloporphyrins. (TTP)SiF₂ readily reacts with excess MeMgBr or LiPh to give (TTP)SiMe₂ or (TTP)SiPh₂, respectively, in contrast to related hexacoordinate *cis*-difluorosilanes which do not react with strong nucleophiles. The enhanced reactivity of (TTP)SiF₂ may be a combination of a *trans*-effect, even though the structural parameters for *cis* and *trans* Si–F bonds and Si–N bonds are essentially the same, and a single-electron transfer process involving the porphyrin ligand.

Introduction

The tendency for silicon to undergo hypercoordination leads to a rich reaction chemistry that yields both novel silane complexes and synthetically useful reagents. A considerable amount of research has been directed at the preparation of penta- and hexacoordinate compounds of silicon that model the intermediates and transition states involved in nucleophilic substitutions at silicon.^{3–8} In the course of these studies, the model complexes themselves have exhibited intriguing chemical and physical behavior.

Neutral hexacoordinate silicon species are prepared by inter- and intramolecular coordination of Lewis bases.^{3,9–12} Corriu and co-workers have done extensive research on substituted-

aryl silicon compounds where the σ -bound aryl contains a pendant moiety capable of dative bonding to the silicon.^{13–19} Confirmation of a hexacoordinate environment around silicon has been made using ¹H and ²⁹Si NMR experiments, but X-ray crystallography has revealed that the tetrahedral environment about silicon is largely preserved. For example, compounds such as (Np')₂SiX₂ and (Np')(Ar')SiF₂ (X = Cl, F; Np' = C₁₀H₆-NMe₂, Ar' = C₆H₄CH₂NMe₂) are formally bicapped tetrahedrons,¹⁷ which exhibit nondissociative fluxional behavior on the NMR time scale.¹⁶

The vast majority of hexacoordinate silicon complexes have reactive ligands disposed in a mutually *cis* geometry. Porphyrins^{20–25} and phthalocyanines^{23,26} are macrocyclic ligands which provide a restricted geometry where the non-nitrogen

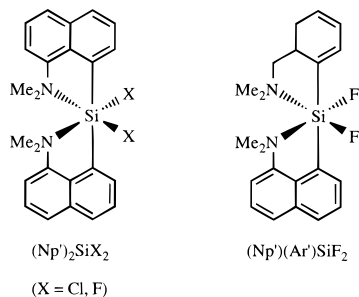
[†] Current address: Department of Chemistry, University of Idaho, Moscow, ID 83844.

[‡] To whom correspondence concerning the X-ray structure determinations should be addressed.

[⊗] Abstract published in *Advance ACS Abstracts*, March 1, 1997.

- (1) This report contains portions from the Ph.D. dissertation of K.M.K.²
- (2) Kane, K. M. Dissertation, Ohio University, 1996.
- (3) Tandura, S. N.; Alekseev, N. V.; Voronkov, M. G. *Top. Curr. Chem.* **1986**, *131*, 99–189.
- (4) Corriu, R. J. P.; Young, J. C. In *The Silicon-Heteroatom Bond*; Patai, S., Rappaport, Z., Eds.; John Wiley & Sons: New York, 1991; pp 49–66.
- (5) Corriu, R. J. P.; Young, C. J. In *The Chemistry of Organic Silicon Compounds*; Patai, S., Rappaport, Z., Eds.; John Wiley & Sons: New York, 1989; pp 1241–1288.
- (6) Kumada, M.; Tamao, K.; Yoshida, J. I. *J. Organomet. Chem.* **1982**, *239*, 115–132.
- (7) Bassindale, A. G.; Taylor, P. G. In *The Chemistry of Organic Silicon Compounds*; Patai, S., Rappaport, Z., Eds.; John Wiley and Sons: New York, 1989; pp 839–892.
- (8) Sheldrick, W. S. In *The Chemistry of Organic Silicon Compounds*; Patai, S., Rappaport, Z., Eds.; John Wiley and Sons: New York, 1989; pp 227–303.

- (9) Klebe, G.; Tran Qui, D. *Acta Crystallogr.* **1984**, *C40*, 476–479.
- (10) Adley, A. D.; Bird, P. H.; Fraser, A. R.; Onyszczuk, M. *Inorg. Chem.* **1972**, *11*, 1402–1409.
- (11) Kummer, D.; Balkir, A.; Köster, H. *J. Organomet. Chem.* **1979**, *178*, 29–54.
- (12) Campbell-Ferguson, H. J.; Ebsworth, E. A. V. *J. Chem. Soc. A* **1967**, 705–712.
- (13) Brelière, C.; Corriu, R. J. P.; Royo, G.; Man, W. C.; Zwecker, J. *Organometallics* **1990**, *10*, 2633–2635.
- (14) Carré, F.; Chuit, C.; Corriu, R. J. P.; Mehdi, A.; Reyé, C. *Angew. Chem., Int. Ed. Engl.* **1994**, *33*, 1097–1099.
- (15) Chuit, C.; Corriu, R. J. P.; Reyé, C.; Young, J. C. *Chem. Rev.* **1993**, *93*, 1371–1448.
- (16) Brelière, C.; Corriu, R. J. P.; Royo, G.; Zwecker, J. *Organometallics* **1989**, *8*, 1834–1836.
- (17) Brelière, C.; Carré, F.; Corriu, R. J. P.; Poirier, M.; Royo, G.; Zwecker, J. *Organometallics* **1989**, *8*, 1831–1833.
- (18) Brelière, C.; Carré, F.; Corriu, R. J. P.; Royo, G. *Organometallics* **1988**, *7*, 1006–1008.
- (19) Carré, F.; Cerveau, G.; Chuit, C.; Corriu, R. J. P.; Réyé, C. *Angew. Chem., Int. Ed. Engl.* **1989**, *28*, 489–491.
- (20) Hoard, J. L. *Ann. N.Y. Acad. Sci.* **1973**, *206*, 18–31.
- (21) Hoard, J. L. *Science* **1971**, *174*, 1295–1302.



ligands are in a *trans* configuration. Although there are numerous examples of germanium(IV)^{27–38} and tin(IV)^{31,33,34,39–57} porphyrin complexes, there were only four reports of silicon(IV)^{31,58–60} porphyrin complexes prior to our work. We recently reported a high-yield route toward the synthesis of the

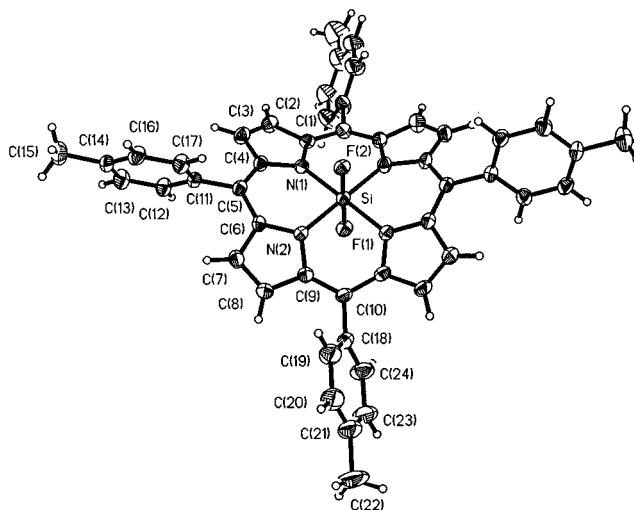


Figure 1. Perspective view of the molecular structure of (TTP)SiF₂·Et₂O with atom labels provided for all unique non-hydrogen atoms. The unlabeled atoms are related to labeled atoms by the crystallographic C₂ axis along F(1)–Si–F(2). The thermal ellipsoids are scaled to enclose 30% probability, and the diethyl ether molecule has been omitted for clarity. Selected bond distances (Å): Si–F(1) 1.650(2); Si–F(2) 1.636(2); Si–N(1) 1.925(2); Si–N(2) 1.911(2). Selected bond angles (deg): F(1)–Si–F(2) 180.00; F(1)–Si–N(1) 89.29(7); F(1)–Si–N(2) 90.01(7); F(2)–Si–N(1) 90.71(7); F(2)–Si–N(2) 89.99(7); N(1)–Si–N(2) 90.02(8); N(1)–Si–N(2') 89.98(8); N(1)–Si–N(1') 178.59(14); N(2)–Si–N(2') 179.98(14).

- (22) Buchler, J. In *Porphyrins and Metalloporphyrins*; Smith, K. M., Ed.; Elsevier: Amsterdam, 1975.
- (23) Sayer, P.; Gouterman, M.; Connell, C. R. *Acc. Chem. Res.* **1982**, *15*, 73–79.
- (24) Scheidt, W. R. In *The Porphyrins*; Dolphin, D., Ed.; Academic Press, Inc.: New York, 1978; Vol. 3; pp 463–511.
- (25) Dolphin, D., Ed. *The Porphyrins*; Academic Press, Inc.: New York, 1978.
- (26) Thomas, A. L. *Phthalocyanine Research and Applications*; CRC Press: Boca Raton, FL, 1990.
- (27) Miyamoto, T. K.; Sugita, N.; Matsumoto, Y.; Sasaki, Y.; Konno, M. *Chem. Lett.* **1983**, 1695–1698.
- (28) Balch, A. L.; Cornman, C. R.; Olmstead, M. M. *J. Am. Chem. Soc.* **1990**, *112*, 2963–2969.
- (29) Guillard, R.; Barbe, J.; Boukhris, M.; Lecomte, C. *J. Chem. Soc., Dalton Trans.* **1988**, 1921–1925.
- (30) Guillard, R.; Barbe, J.; Boukhris, A.; Lecomte, C.; Anderson, J. E.; Xu, Q. Y.; Kadish, K. M. *J. Chem. Soc., Dalton Trans.* **1988**, 1109–1113.
- (31) Gouterman, M.; Schwartz, F. P.; Smith, P. D.; Dolphin, D. *J. Chem. Phys.* **1973**, *59*, 676–690.
- (32) Kadish, K. M.; Xu, Q. Y.; Barbe, J.; Anderson, J. E.; Wang, E.; Guillard, R. *J. Am. Chem. Soc.* **1987**, *109*, 7705–7714.
- (33) Barbe, J.; Guillard, R.; Lecomte, C.; Gerardin, R. *Polyhedron* **1984**, *3*, 889–894.
- (34) Cloutour, C.; Lafargue, D.; Richards, J. A.; Pommier, J. *J. Organomet. Chem.* **1977**, *137*, 157–163.
- (35) Mavridis, A.; Tulinsky, A. *Inorg. Chem.* **1976**, *15*, 2723–2727.
- (36) Kane, A. R.; Yalman, R. G.; Kenney, M. E. *Inorg. Chem.* **1968**, *7*, 2588–2592.
- (37) Cloutour, C.; Lafargue, D.; Pommier, J. C. *J. Organomet. Chem.* **1980**, *190*, 35–42.
- (38) Maiya, G. B.; Barbe, J.; Kadish, K. M. *Inorg. Chem.* **1989**, *28*, 2524–2527.
- (39) Arnold, D. P.; Bartley, J. P. *Inorg. Chem.* **1994**, *33*, 1486–1490.
- (40) Barbe, J.; Ratti, C.; Richard, P.; Lecomte, C.; Gerardin, R.; Guillard, R. *Inorg. Chem.* **1990**, *29*, 4126–4130.
- (41) Arnold, D. P. *Polyhedron* **1988**, *7*, 2225–2227.
- (42) Smith, G.; Arnold, D. P.; Kennard, C. H. L.; Mak, T. C. W. *Polyhedron* **1991**, *10*, 509–516.
- (43) Cullen, D. L.; Meyer, E. F., Jr. *Acta Crystallogr.* **1973**, *B29*, 2507–2515.
- (44) Lin, H.; Chen, J.; Hwang, L. *Aust. J. Chem.* **1991**, *44*, 747–751.
- (45) Collins, D. M.; Scheidt, W. R.; Hoard, J. L. *J. Am. Chem. Soc.* **1972**, *94*, 6689–6696.
- (46) Kato, S.; Noda, I.; Mizuta, M.; Itoh, Y. *Angew. Chem., Int. Ed. Engl.* **1979**, *18*, 82–3.
- (47) Noda, I.; Kato, S.; Mizuta, M.; Yasuoka, N.; Kasai, N. *Angew. Chem., Int. Ed. Engl.* **1979**, *18*, 83.
- (48) Guillard, R.; Barbe, J. M.; Fahim, M.; Atmani, A.; Moninot, G.; Kadish, K. M. *New J. Chem.* **1992**, *16*, 815–820.
- (49) Arnold, D. P.; Morrison, E. A.; Hanna, J. V. *Polyhedron* **1990**, *10*, 1331–1336.
- (50) Arnold, D. P. *Polyhedron* **1986**, *5*, 1957–1963.
- (51) Kadish, K. M.; Xu, Q. Y.; Maiya, G. B.; Barbe, J.; Guillard, R. *J. Chem. Soc., Dalton Trans.* **1989**, 1531–1536.
- (52) Milgrom, L. R.; Sheppard, R. N. *J. Chem. Soc., Chem. Commun.* **1985**, 350–351.
- (53) Arnold, D. P.; Tiekink, E. R. *Polyhedron* **1995**, *14*, 1785–1789.
- (54) Onaka, S.; Kondo, Y.; Yamashita, M.; Tatematsu, Y.; Kato, Y.; Goto, M.; Ito, T. *Inorg. Chem.* **1985**, *24*, 1070–1076.
- (55) Guillard, R.; Ratti, C.; Barbe, J.; Dubois, D.; Kadish, K. M. *Inorg. Chem.* **1991**, *30*, 1537–1542.

novel (porphyrinato)silicon(IV) complexes (TTP)SiX₂ (TTP = the dianion of tetra-*p*-tolylporphyrin; X = Cl, F, O₃SCF₃) and the first X-ray structure of a silicon porphyrin that confirmed the *trans* geometry of the triflate groups.⁶¹ We now report the X-ray crystal structures of the difluoro(porphyrinato)silicon(IV) complexes (TTP)SiF₂·Et₂O and (TTFP)SiF₂ (TTFP = the dianion of tetrakis(*p*-(trifluoromethyl)phenyl)porphyrin) and a structural comparison of these complexes to other main group metalloporphyrins. We also report the unprecedented nucleophilic substitution of the hexacoordinate difluorosilane (TTP)SiF₂.

Results and Discussion

Structures of (TTP)SiF₂·Et₂O and (TTFP)SiF₂. Perspective views of (TTP)SiF₂, as a diethyl ether solvate, and (TTFP)SiF₂ with the atom-labeling schemes are shown in Figures 1 and 2, respectively. A diagram of the carbon–nitrogen cores for (TTP)SiF₂ and (TTFP)SiF₂ illustrating important bond distances and angles is shown in Figure 3. The structures of (TTP)SiF₂ and (TTFP)SiF₂ exhibit many similarities. The two fluorine atoms are in a *trans* orientation, and the porphyrin rings show deformation into a saddle shape. Each molecule has a crystallographically imposed C₂ axis which coincides with the F(1)–Si–F(2) axis. The Si–F and Si–N distances in both complexes are essentially the same with average distances of 1.642 ± 0.011 and 1.919 ± 0.007 Å, respectively. The F–Si–N angles average 90.00 ± 0.77°, resulting in a near-

- (56) Kadish, K. M.; Swistak, C.; Boisselier-Cocolios, B.; Barbe, J. M.; Guillard, R. *Inorg. Chem.* **1986**, *25*, 4336–4343.
- (57) Cloutour, C.; Lafargue, D.; Pommier, J. C. *J. Organomet. Chem.* **1978**, *161*, 327–334.
- (58) Kadish, K. M.; Xu, Q. Y.; Barbe, J.; Guillard, R. *Inorg. Chem.* **1988**, *27*, 1191–1198.
- (59) Buchler, J. W.; Puppe, L.; Rohbock, K.; Schneehage, H. H. *Chem. Ber.* **1973**, *106*, 2710–2732.
- (60) Marriot, P. J.; Gill, J. P.; Eglinton, G. *J. Chromatogr.* **1982**, *249*, 291–310.
- (61) Kane, K. M.; Lemke, F. R.; Petersen, J. L. *Inorg. Chem.* **1995**, *34*, 4085–4091.

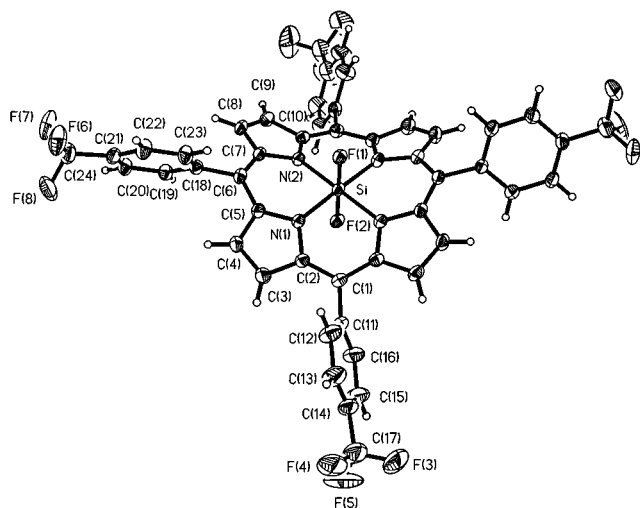


Figure 2. Perspective view of the molecular structure of (TTFP)SiF₂ with atom labels provided for all unique non-hydrogen atoms. The unlabeled atoms are related to labeled atoms by the crystallographic C₂ axis along F(1)–Si–F(2). The thermal ellipsoids are scaled to enclose 30% probability. Selected bond distances (Å): Si–F(1) 1.628(2); Si–F(2) 1.652(2); Si–N(1) 1.9154(13); Si–N(2) 1.924(2). Selected bond angles (deg): F(1)–Si–F(2) 180.0; F(1)–Si–N(1) 91.14(6); F(1)–Si–N(2) 90.50(5); F(2)–Si–N(1) 88.86(6); F(2)–Si–N(2) 89.50(5); N(1)–Si–N(2) 89.91(6); N(1)–Si–N(2') 90.07(6); N(1)–Si–N(1') 177.72(11); N(2)–Si–N(2') 179.00(11).

perfect octahedral environment about the silicon atom. The four pyrrole nitrogens have a mean deviation from planarity of ± 0.012 Å in (TTP)SiF₂ and ± 0.011 Å in (TTFP)SiF₂. The silicon atom is 0.012 Å above the N₄ plane in (TTP)SiF₂ while in (TTFP)SiF₂ this deviation is 0.028 Å.

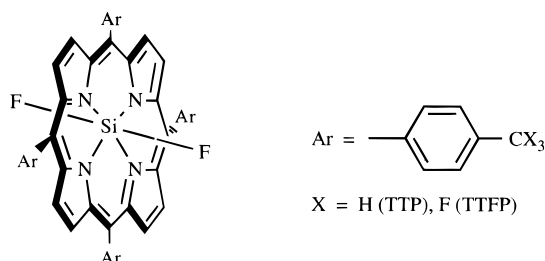


Figure 3. Diagram of the carbon–nitrogen skeletons for (TTP)SiF₂ (top) and (TTFP)SiF₂ (bottom) showing important bond distances (in Å) and bond angles (in deg).

Table 1. Selected Structural Data (Interatomic Distances (Å)) for Hexacoordinate Fluorosilanes

bond	(TTP)- SiF ₂	(TTFP)- SiF ₂	<i>trans</i> - (py) ₂ SiF ₄ ^a	<i>cis</i> - (bipy) ₂ SiF ₄ ^b	(Ar')(Np')- SiF ₂ ^c
Si–N	1.925 1.911	1.924 1.915	1.93	1.975	2.665 2.806
Si–F	1.650 1.636	1.652 1.628	1.64	1.655 1.635	1.604 1.617

^a py = pyridine; ref 12. ^b bipy = bipyridine; ref 10. ^c Ar' = C₆H₄CH₂NMe₂; Np' = C₁₀H₆NMe₂; ref 17.

The pyrrole groups are essentially planar, with deviations from planarity of ± 0.015 Å in (TTP)SiF₂ and ± 0.014 Å in (TTFP)SiF₂, and have average dihedral angles of 18.3° in (TTP)SiF₂ and 21.2° in (TTFP)SiF₂, with respect to the N₄ plane. Since the pyrrole groups are planar, the deformation of the porphyrin ring is manifested in displacement of the *meso* carbons above and below the N₄ plane (+0.656 and –0.602 Å in (TTP)SiF₂ and +0.668 and –0.663 Å in (TTFP)SiF₂). This amounts to a “twisting” of the pyrrole rings about an axis containing the N atom and the center of the C_β–C_β bond of each pyrrole, and this type of deformation gives a *ruf* nonplanar porphyrin, according to the formalism of Scheidt and Lee.⁶² The deformation arises from the porphyrin contracting to accommodate the small central silicon atom and is consistent with other small-atom metalloporphyrin structures.

The most striking feature of these two difluorosilicon porphyrins is the similarity of the Si–F bond lengths. In spite

of the more electron-donating tolyl groups on the porphyrin ring in (TTP)SiF₂, the average Si–F distance of 1.64 Å is identical to the average Si–F distance in (TTFP)SiF₂, which has *p*-(trifluoromethyl)phenyl groups on the periphery of the porphyrin ring. The insensitivity of Si–F bonds to the electron-donating ability of other ligands is reasonable given the high strength of silicon–fluorine bonds.^{66,67}

Table 1 presents some selected data from the X-ray crystal structures of (Por)SiF₂ (Por = TTP, TTFP) and related hexacoordinate fluorosilanes. The Si–F bond distances of the (Por)SiF₂ complexes are within the range of the Si–F bond distances

(62) Scheidt, W. R.; Lee, Y. J. *Struct. Bonding* **1987**, *64*, 1–70.

(63) Hoard, J. L. In *Porphyrins and Metalloporphyrins*; Smith, K. M., Ed.; Elsevier: Amsterdam, 1975.

(64) Meyer, E. F., Jr.; Cullen, D. In *The Porphyrins*; Academic Press: New York, 1978; Vol. 3; pp 513–529.

(65) Smith, P. D.; James, B. R.; Dolphin, D. H. *Coord. Chem. Rev.* **1981**, *39*, 31–75.

(66) Ebsworth, E. A. V. *Volatile Silicon Compounds*; Pergamon: Oxford, U.K., 1963; Vol. 4.

(67) Van Dyke, C. H. *The Bond to Halogens and Halogenoids*; Marcel Dekker: New York, 1972; Vol. 2.

Table 2. Selected Structural Data for Group 14 Metalloporphyrins

	(TTP)Si(OTf) ₂ ^a	(TTFP)SiF ₂	(TTP)SiF ₂	(OEP)GeF ₂ ^b	(TPP)SnF ₂ ^c	[(TPP)Sn(H ₂ O) ₂] ⁺ ^d
	Average Bond Distances ^e (Å)					
M–F		1.64	1.64	1.79	1.95	
M–N	1.87	1.92	1.92	1.97	2.06	2.06
C _m –C _m (<i>trans</i>)	6.46	6.58	6.61	6.70	6.84	6.82
dev of C _m from N ₄ plane	±0.79	±0.67	±0.63	±0.44	planar	planar
	Average Bond Angles ^e (deg)					
C _α –C _m –C _α	120.1	121.7	121.5	125.5	126.9	130.3
dihedral angle of pyrroles	25.1	21.2	18.3	19.8	planar	planar

^a Reference 61. ^b OEP = dianion of octaethylporphyrin; ref 30. ^c Reference 53. ^d As the triflate salt; ref 42. ^e C_m = *meso* carbon; C_α = pyrrole α -carbon.

for the other hexacoordinate difluorosilanes. Moreover, the Si–F bond lengths appear to be invariant with disposition about the silicon atom; therefore, no *trans* effect is discernible in the structural data for (Por)SiF₂ when compared to comparable *cis*-difluorosilanes. The average Si–F bond distance, for all five complexes, is 1.635 ± 0.017 Å. However, the Si–F distances in (Ar')(Np')SiF₂¹⁷ are noticeably shorter than the average.

A significant difference is also found in the Si–N interatomic separations of (Ar')(Np')SiF₂, which are 0.75–0.85 Å longer than the average Si–N bond distance (1.930 ± 0.021 Å) for the other four difluorosilane complexes. Although (Ar')(Np')-SiF₂ is considered to be hexacoordinate, the Si–N dative bonding interaction is extremely weak. This is reflected in the reported *J*_{SiF} for (Ar')(Np')SiF₂ (273 Hz),¹⁷ which is significantly larger than *J*_{SiF} for (TTP)SiF₂ (203 Hz)^{61,68} and (TTFP)SiF₂ (205 Hz),^{2,68} consistent with the short Si–F bond in (Ar')(Np')SiF₂ and the longer Si–F bonds in (Por)SiF₂. Indeed, the angles around silicon in (Ar')(Np')SiF₂ were reported to be more consistent with a bicapped tetrahedron than with an octahedral geometry.⁶⁹

Comparison of (TTP)SiF₂ and (TTFP)SiF₂ with Other Main-Group Porphyrin Complexes. Nonplanar porphyrins have been the subject of increasing study of late because of the effects on the reactivity of the central atom and the porphyrin that these distortions cause.^{27,70–74} It is clear that the porphyrin moiety is a rather flexible ligand, and the ability to present nonplanar conformations has been attributed to the biological activity of some metalloporphyrins.⁷²

Table 2 contains selected structural data for several group 14 metalloporphyrin complexes. An important comparison can be made between the molecular structures of (Por)SiF₂ (Por = TTP, TTFP) and the structure of (TTP)Si(OTf)₂ (OTf = O₃-SCF₃).⁶¹ The Si–N bond length is shorter in the triflate derivative than for the difluoro derivatives. We reported that the Si–O bond length of (TTP)Si(OTf)₂ was quite long and is consistent with the observed facile displacement of the triflates (*vide supra*). This would also be consistent with a greater

positive charge on the silicon, resulting in a greater bonding interaction between the pyrrole nitrogens and the silicon and, thus, a shorter Si–N distance. The effect on the porphyrin would be a larger degree of deformation as the porphyrin contracts on the cationic silicon. Conversely, the tendency of fluorine to participate as a π -donor to silicon should decrease the electropositive character of the silicon atom, thereby lessening the Si–N interaction. An increase in the Si–N bond distance occurs with a concomitant decrease in deformation of the porphyrin core.

This trend in silicon–porphyrin bonding is clearly evident from the structural data (Table 2). The smaller amount of deformation in the structures of (Por)SiF₂ can be measured by the *trans* C_m–C_m distances and the C_α–C_m–C_α angles, both of which are greater than those observed in (TTP)Si(OTf)₂. The same trend is observed in the crystal structures of the *trans* alkylphosphorus porphyrin complexes (OEP)P(O)Et and [(OEP)P(OH)Et][ClO₄].⁷⁵ The P=O bond involves sufficient π -back-bonding from oxygen to phosphorus that the porphyrin ligand in (OEP)P(O)Et is planar, whereas the structure of [(OEP)P(OH)Et]⁺ (with a P–O bond) shows a more ruffled macrocycle. The difference in porphyrin deformation for the (porphyrinato)-silicon complexes parallels that observed for the (porphyrinato)-phosphorus complexes, where the M–N distances are longer in the more planar complexes (Table 1; P–N = 1.884 Å in (OEP)P(O)Et, and 2.001 Å in [(OEP)P(OH)Et]⁺).

Tin(IV) metalloporphyrins are invariably planar molecules (Table 2); despite the larger size of the tin metal atom compared to silicon, it is still small enough to fit in the core of the porphyrin. On the other hand, structural studies of germanium porphyrin complexes have revealed that both planar and nonplanar conformations exist, as germanium is small enough to induce deformation of the macrocycle, but the steric and electronic requirements of the axial ligands may limit this ruffling. Within group 14, an increase in the size of the metal decreases the ruffling of the porphyrin with respect to the N₄ plane.

As noted before, the pyrroles remain essentially unchanged (planar), so deformation of the porphyrin must occur at the *meso* carbons (Table 2). The most noticeable changes are seen in the M–N and *trans* C_m–C_m distances, which all gradually increase to a maximum in the planar tin porphyrin complexes. In addition, as the metal size is increased, the axial displacements of the *meso* carbons decrease, as do the dihedral angles of the pyrroles with respect to the N₄ plane. Moreover, the angle at the *meso* carbon (C_α–C_m–C_α) for all of the complexes gradually increases from 120 to 130° as the central atom becomes larger and the metalloporphyrin becomes planar.

Reactivity of (TTP)SiF₂ toward Nucleophilic Substitution: *Trans* Influence? The difluorosilane (Np')₂SiF₂ has been

(68) Kane, K. M.; Lorenz, C. R.; Heilman, D. M.; Lemke, F. R. *Inorg. Chem.* **1997**, submitted for publication.

(69) The geometry around silicon in (Np')(Ar')SiF₂ is best described as tetrahedral [bond angles: F–Si–F (96.5°), C(Np')–Si–C(Ar') (135.5°), C(Np')–Si–F (104.5°, 103.3°), and C(Ar')–Si–F (108.5°, 101.8°)] with the two nitrogen atoms capping a face of the tetrahedron *trans* to the fluorine atoms [N–Si–F average 175°].¹⁷

(70) Hancock, R. D.; Weaving, J. S.; Marques, H. M. *J. Chem. Soc., Chem. Commun.* **1989**, 1176–1178.

(71) Munro, O. Q.; Bradley, J. C.; Hancock, R. D.; Marques, H. M.; Marsicano, F.; Wade, P. W. *J. Am. Chem. Soc.* **1992**, *114*, 7218–7230.

(72) Ravikanth, M.; Chandrashekar, T. K. *Struct. Bonding* **1995**, *82*, 105–188.

(73) Renner, M. W.; Barkigia, K. M.; Zhang, Y.; Medforth, C. J.; Smith, K. M.; Fajer, J. *J. Am. Chem. Soc.* **1994**, *116*, 8582–8592.

(74) Sparks, L. D.; Medforth, C. J.; Park, M.; Chamberlain, J. R.; Ondrias, M. R.; Senge, M. O.; Smith, K. M.; Shelnut, J. A. *J. Am. Chem. Soc.* **1993**, *115*, 581–592.

(75) Yamamoto, Y.; Nadano, R.; Itagaki, M.; Akiba, K. *J. Am. Chem. Soc.* **1995**, *117*, 8287–8288.

reported to be unreactive toward strong nucleophiles, in sharp contrast to the ease of substitution of the analogous dichlorosilane $(\text{Np}')_2\text{SiCl}_2$.¹³ On the basis of the crystal structure of $(\text{Ar}')(\text{Np}')\text{SiF}_2$, which has somewhat short Si–F bond lengths for hexacoordinate silicon (*vide infra*; Table 1), it was concluded that $(\text{Np}')_2\text{SiF}_2$ had similar Si–F bond distances. The inertness of $(\text{Np}')_2\text{SiF}_2$ toward nucleophilic substitution was attributed to the combination of unstretched Si–F bonds and steric congestion about silicon.

Because the fluorine atoms in $(\text{Ar}')(\text{Np}')\text{SiF}_2$ and $(\text{Np}')_2\text{SiF}_2$ are mutually *cis*, we were interested if a *trans* influence could be observed in the *trans*-difluorosilane $(\text{TTP})\text{SiF}_2$. The Si–F distances in $(\text{Ar}')(\text{Np}')\text{SiF}_2$ and $(\text{TTP})\text{SiF}_2$ are similar (1.61 and 1.64 Å, respectively), and Corriu's conclusion¹³ that hexacoordinate fluorosilanes are substitutionally inert was supported by our own observation that $(\text{TTP})\text{SiF}_2$ was unreactive toward water. However, red toluene solutions of $(\text{TTP})\text{SiF}_2$ react with MeMgBr within seconds to give green solutions of $(\text{TTP})\text{SiMe}_2$. The stoichiometry of $(\text{TTP})\text{SiMe}_2$ was confirmed by a singlet at -7.55 ppm integrating for 6 hydrogens in the ^1H NMR spectrum. Isolation of pure $(\text{TTP})\text{SiMe}_2$ was complicated by the photosensitivity of the Si–Me bonds under ambient lighting.⁷⁶ Similar results were observed when $(\text{TTP})\text{SiF}_2$ was reacted with LiPh to afford the diphenyl analogue, which is also photosensitive.² Based on the observed reactivity of $(\text{TTP})\text{SiF}_2$ toward strong nucleophiles, it is reasonable to suspect that a *trans* influence is operative; however, the similarity of the Si–F distances for $(\text{Ar}')(\text{Np}')\text{SiF}_2$ and $(\text{TTP})\text{SiF}_2$ suggests that a *trans* influence is not solely responsible for the reactivity of the porphyrin complex and the inertness of Corriu's difluorosilane.

The ease by which porphyrin complexes can be reduced may also play a role in the nucleophilic substitution of $(\text{TTP})\text{SiF}_2$. A mechanistic study⁵⁷ of the reaction of Grignard reagents with germanium and tin porphyrin complexes showed that single-electron transfer (SET) from the alkylmagnesium to the porphyrin ring occurs to generate an intermediate radical anion, in which the unpaired electron was postulated to reside in the macrocycle or on the metal. The loss of an axial ligand as an anion to generate a porphyrin radical was not specifically identified, but this is a reasonable outcome. Additional evidence of SET from a carbanion to a porphyrin is suggested by the observation⁷⁷ that the reaction of $(\text{TPP})\text{FeCl}$ with even a slight excess of lithium acetylide caused reduction of the iron center to Fe(II). Moreover, the electron-withdrawing ability of the axial fluorides in $(\text{Por})\text{SiF}_2$, compared to other axial groups, has been shown to facilitate the electrochemical reduction of the porphyrin ring relative to axial chlorides.⁷⁸

Conclusion

The molecular structures of $(\text{Por})\text{SiF}_2$ (Por = TTP, TTFP) provide further information on the bonding characteristics of hexacoordinate silicon complexes where a strict *trans* geometry is imposed. In addition, the structures of $(\text{Por})\text{SiF}_2$ complete a homologous series of structurally characterized group 14 difluorometalporphyrins $(\text{Por})\text{MF}_2$ (M = Si, Ge, Sn; Por = TTP, TTFP, TPP, OEP). Although the Si–F bond lengths observed in these difluoro(porphyrinato)silicon(IV) complexes do not differ appreciably from similar *cis*- and *trans*-difluo-

rosilanes, the unprecedented nucleophilic substitution observed for $(\text{TTP})\text{SiF}_2$ may be a consequence of this *trans* geometry of the fluorides. Although there are no reports on the reactivity of $(\text{py})_2\text{SiF}_4$ ¹² and $(\text{bipy})\text{SiF}_4$ ¹⁰ toward nucleophiles, the probable contribution of the porphyrin ring cannot be ignored as the reason for the enhanced reactivity of $(\text{TTP})\text{SiF}_2$.

Experimental Section

General Procedures. All manipulations of oxygen- or water-sensitive compounds were carried out either under an atmosphere of argon by using Schlenk or vacuum-line techniques or under a helium/argon atmosphere in a Vacuum Atmospheres drybox. ^1H NMR (400 and 250 MHz) and $^{19}\text{F}\{^1\text{H}\}$ NMR (376 and 235 MHz) spectra were recorded on a Varian VXR 400S and a Bruker AC-250 spectrometer, respectively, at 295 K. ^{29}Si NMR (79.5 MHz) spectra were recorded on a Varian VXR 400S spectrometer at 295 K. The ^1H chemical shifts were referenced to the residual proton peak of the solvent: $\text{C}_6\text{D}_5\text{H}$, δ 7.15, and CDHCl_2 , δ 5.32. The ^{19}F chemical shifts were referenced to external $\text{CF}_3\text{CO}_2\text{H}$ (δ 0.00). The ^{29}Si chemical shifts were referenced to external SiMe_4 (δ 0.00).

Materials. $(\text{TTP})\text{SiF}_2$ was prepared as reported previously.⁶¹ $(\text{TTFP})\text{SiF}_2$ was prepared in a manner similar to $(\text{TTP})\text{SiF}_2$. Spectroscopic data for $(\text{TTFP})\text{SiF}_2$ are as follows: ^1H NMR (CD_2Cl_2) δ 9.87 (s, 8H, pyrrole CH), 8.27 (d, $J_{\text{HH}} = 7.9$ Hz, 8H, $\text{C}_6\text{H}_4\text{CF}_3$), 8.04 (d, $J_{\text{HH}} = 7.9$ Hz, 8H, $\text{C}_6\text{H}_4\text{CF}_3$); $^{19}\text{F}\{^1\text{H}\}$ (CD_2Cl_2) δ 13.5 (s, 6F, CF_3), -46.1 (s, 1F, SiF; with ^{29}Si satellites, $J_{\text{SiF}} = 205.0$ Hz). Full synthetic details for the preparation of $(\text{TTFP})\text{SiF}_2$ will be reported in a forthcoming publication.⁶⁸

$(\text{TTP})\text{SiMe}_2$. Toluene (35 mL) was added to a flask containing $(\text{TTP})\text{SiF}_2$ (150 mg, 0.20 mmol), and the solution was stirred under a flow of argon. Methylmagnesium bromide (0.20 mL, 3.0 M in Et_2O) was added dropwise to the solution, which turned from red to green within seconds. After 15 min, 0.5 mL of CH_2Cl_2 was added and the volatiles were removed under vacuum. The flask was transferred to the drybox where the residue was extracted with 50 mL of toluene and filtered through Celite. Evaporation of the filtrate to dryness and drying the residue overnight under vacuum yielded 139 mg of blue-purple powder (83%). ^1H NMR (CD_2Cl_2): δ 8.96 (s, 8H, pyrrole CH), 8.09 (d, $J_{\text{HH}} = 7.9$ Hz, 8H, $\text{C}_6\text{H}_4\text{CH}_3$), 7.58 (d, $J_{\text{HH}} = 7.9$ Hz, 8H, $\text{C}_6\text{H}_4\text{CH}_3$), 2.69 (s, 12H, $\text{C}_6\text{H}_4\text{CH}_3$), -7.55 (s, 6H, SiCH_3). ^{29}Si DEPT NMR (CD_2Cl_2): δ -185 (s).

X-ray Structural Analyses of $(\text{TTP})\text{SiF}_2\cdot\text{Et}_2\text{O}$ and $(\text{TTFP})\text{SiF}_2$. A dark purple crystal of $(\text{TTP})\text{SiF}_2\cdot\text{Et}_2\text{O}$ (grown by slow diffusion of Et_2O vapor into a CH_2Cl_2 solution of $(\text{TTP})\text{SiF}_2$) was removed from a saturated ether solution and sealed in a glass capillary tube containing a drop of the mother liquor, whereas a dark purple crystal of $(\text{TTFP})\text{SiF}_2$ (grown by slow diffusion of Et_2O vapor into a CH_2Cl_2 solution of $(\text{TTFP})\text{SiF}_2$) was wedged and then sealed in a glass capillary tube. The reflections used for the unit cell determination were located and indexed by the automatic peak search routine XSCANS⁷⁹ developed for the Siemens P4 automated diffractometer. For $(\text{TTP})\text{SiF}_2\cdot\text{Et}_2\text{O}$, the lattice parameters and orientation matrix were determined from a nonlinear least-squares fit of the orientation angles of 27 reflections at 22 °C. The systematic absences of $\{hkl\}$, $h + k = 2n + 1$, and $\{h0l\}$, $l = 2n + 1$, are consistent with the noncentrosymmetric space group *Cc* (No. 9, C_s^4) and the centrosymmetric space group $C2/c$ (No. 15, C_{2h}^6). For $(\text{TTFP})\text{SiF}_2$, the corresponding lattice parameters and orientation matrix were determined from a nonlinear least-squares fit of the orientation angles of 38 reflections at 22 °C. The data collection was performed with the nonstandard *I*-centered unit cell ($a = 28.488(3)$ Å, $b = 9.546(1)$ Å, $c = 15.941(1)$ Å, $\beta = 94.41(1)^\circ$) which was later transformed to the standard *C*-centered cell. The systematic absences of $\{hkl\}$, $h + k = 2n + 1$, and $\{h0l\}$, $l = 2n + 1$, are consistent with the noncentrosymmetric space group *Cc* (No. 9, C_s^4) and the centrosymmetric space group $C2/c$ (No. 15, C_{2h}^6). In both cases the centrosymmetric space group was determined to be the correct one on the basis of the structure solution and refinement. The refined lattice parameters and other pertinent crystallographic information are provided in Table 3.

(76) Kadish and co-workers have observed that the alkyl and aryl complexes $(\text{OEP})\text{SiR}_2$ (R = Me, Ph) were sensitive to visible light.⁵⁸

(77) Balch, A. L.; Latos-Grazynski, L.; Noll, B. C.; Phillips, S. L. *Inorg. Chem.* **1993**, *32*, 1124–1129.

(78) Lorenz, C. R.; Dewald, H. H.; Lemke, F. R. *J. Electroanal. Chem.* **1996**, *415*, 179–181.

(79) XSCANS (version 2.0) is a diffractometer control system developed by Siemens Analytical X-ray Instruments, Madison, WI.

Table 3. Crystallographic Data for (TTP)SiF₂·Et₂O and (TTFP)SiF₂

	(TTP)SiF ₂ ·Et ₂ O	(TTFP)SiF ₂
empirical formula	C ₅₂ H ₄₆ F ₂ N ₄ OSi	C ₄₈ H ₂₄ F ₁₄ N ₄ Si
fw	809.02	950.80
cryst system	monoclinic	monoclinic
space group	C2/c	C2/c
<i>a</i> , Å	30.228(4)	31.557(2)
<i>b</i> , Å	9.913(4)	9.546(1)
<i>c</i> , Å	15.474(5)	15.941(1)
α, deg	90	90
β, deg	114.58(3)	115.83(1)
γ, deg	90	90
<i>V</i> , Å ³	4217(2)	4322.4(8)
<i>Z</i>	4	4
ρ(calcd), g cm ⁻³	1.274	1.461
radiation (λ, Å)	Mo Kα (0.710 73)	Mo Kα (0.710 73)
μ, cm ⁻¹	1.09	1.55
<i>T</i> , K	295(2)	295(2)
<i>R</i> 1 ^a	0.0588	0.0489
w <i>R</i> 2 ^b	0.1164	0.1114

$$^a R1 = \sum ||F_o| - |F_c|| / \sum |F_o|. \quad ^b wR2 = [\sum (w_i(F_o^2 - F_c^2)^2) / \sum (w_i(F_o^2)^2)]^{1/2}.$$

Intensity data were measured with graphite-monochromated Mo Kα radiation (λ = 0.710 73 Å) and variable ω scans of 4–10 °/min and 2–10 °/min, respectively. Background counts were measured at the beginning and at the end of each scan with the crystal and counter kept stationary. The intensities of the three standard reflections measured after every 100 reflections for (TTP)SiF₂·Et₂O decreased linearly by ca. 15% during data collection, whereas those measured for (TTFP)SiF₂ did not show any significant variation or decrease over time. The intensity data were corrected for Lorentz–polarization effects and sample decomposition.

Initial atomic coordinates were provided by direct methods (SHELX-TL-IRIS) with the coordinates for the remaining non-hydrogen atoms obtained from subsequent Fourier summations. The crystal structures of (TTP)SiF₂ and (TTFP)SiF₂ are both constrained by a crystallographic 2-fold rotation axis which passes through the Si, F(1), and F(2) atoms. As the refinement of (TTP)SiF₂ progressed, it became apparent that the crystal lattice contained a disordered ether molecule with its central O atom located on a crystallographic inversion center. This disorder was refined with a two-site model keeping the O–C(CH₂), C(CH₂)–C(CH₃), and O–C(CH₃) interatomic distances restrained at 1.43 ± 0.02, 1.54 ± 0.02, and 2.30 ± 0.02 Å. No significant intermolecular interactions between Et₂O and the (TTP)SiF₂ were observed. In contrast for (TTFP)SiF₂, the appearance of residuals of electron density between the refined positions of the six fluorine atoms of the two CF₃ substituents indicated these groups are partially disordered. This disorder was modeled by restraining the three C(17)–F and three C(14)–F distances to 1.32 ± 0.02 Å and the interatomic F–F distances to 2.12 ± 0.02 Å. The unprimed F atoms (F(3)–F(8)) were refined anisotropically,

whereas the primed F atoms (F(3′)–F(8′)) were refined isotropically with their temperature factors constrained to be equal within each CF₃ group. The refinement of the occupancy factor for the unprimed F and primed F atoms indicated a 90:10 disorder for these atoms. Idealized positions for all of the hydrogen atoms were included as fixed contributions using a riding model with isotropic temperature factors set at 1.2 times that of the adjacent carbon. The positions of the methyl hydrogens were optimized by a rigid rotating group refinement with idealized tetrahedral angles. Full-matrix least-squares refinement, based upon the minimization of $\sum w_i |F_o^2 - F_c^2|$, with $w_i^{-1} = [\sigma^2(F_o^2) + (aP)^2 + bP]$ where $P = (\max(F_o^2, 0) + 2F_c^2)/3$, was performed with SHELXL-93⁸⁰ operating on a Silicon Graphics IRIS Indigo workstation. The values of *a* and *b* are 0.063, 0.000 and 0.0559, 5.19 for (TTP)SiF₂·Et₂O and (TTFP)SiF₂, respectively. The final discrepancy indices⁸¹ are provided in Table 3. Difference electron density maps did not reveal any significant residuals on electron density in either case.

The refined atomic coordinates (×10⁴) for (TTP)SiF₂·Et₂O and (TTFP)SiF₂ are given in the Supporting Information along with a complete listing of the interatomic distances and bond angles. The values of the anisotropic thermal displacement parameters for all the non-hydrogen atoms and the idealized coordinates for the hydrogen atoms in the corresponding crystallographic asymmetric unit are also included for these two compounds.

Acknowledgment. F.R.L. and K.M.K. acknowledge the financial support of the Petroleum Research Fund, administered by the American Chemical Society (Grant No. 26059-G3), the Ohio University Condensed Matter and Surface Science Program, and the John Houk Memorial Research Fund (Ohio University). J.L.P. acknowledges the Chemical Instrumentation Program of the National Science Foundation (Grant No. CHE-9120098) for acquisition of a Siemens P4 X-ray diffractometer. We thank Drs. E. Tiekink (University of Adelaide, Adelaide, Australia) and D. Arnold (Queensland University of Technology, Brisbane, Australia) for providing additional structural data.

Supporting Information Available: Text describing X-ray procedures and complete listings of crystallographic data, positional parameters, bond lengths and angles, thermal parameters, and atomic parameters of hydrogen atoms for (TTP)SiF₂·Et₂O and (TTFP)SiF₂ (18 pages). Ordering information is given on any current masthead page.

IC960639X

- (80) SHELXL-93 is a FORTRAN-77 program (Professor G. Sheldrick, Institut für Anorganische Chemie, University of Göttingen, D-37077 Göttingen, Germany) for single-crystal X-ray structural analyses.
- (81) The discrepancy indices were calculated from the expressions $R1 = \sum ||F_o| - |F_c|| / \sum |F_o|$ and $wR2 = [\sum (w_i(F_o^2 - F_c^2)^2) / \sum (w_i(F_o^2)^2)]^{1/2}$, and the standard deviation of an observation of unit weight (GOF) is equal to $[\sum (w_i(F_o^2 - F_c^2)^2) / (n - P)]^{1/2}$, where *n* is the number of reflections and *P* is the number of parameters varied during the last refinement cycle.